

AD-A142 555

RARE-EARTH ION-HOST LATTICE INTERACTIONS: 15 ANALYSIS
OF THE SPECTRA OF Nd^{3+} IN $\text{Gd}_3\text{Sc}_2\text{Ga}_3\text{O}_{12}$ (U) HARRY DIAMOND
LABS ADELPHI MD C A MORRISON ET AL. MAY 84 HDL-TR-2035

1/1

UNCLASSIFIED

F/G 7/4

NL



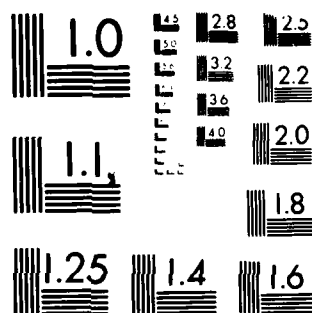
END

DATE

FILED

8-84

DTIC



MICROCOPY RESOLUTION TEST CHART
NATIONAL BUREAU OF STANDARDS-1963-A

AD-A142 555

THIS REPORT CONTAINS MICROFICHE INSERTS

UNCLASSIFIED

SECURITY CLASSIFICATION OF THIS PAGE (When Data Entered)

REPORT DOCUMENTATION PAGE		READ INSTRUCTIONS BEFORE COMPLETING FORM
1. REPORT NUMBER HDL-TR-2035	2. GOVT ACCESSION NO. AD-A142555	3. RECIPIENT'S CATALOG NUMBER
4. TITLE (and Subtitle) Rare-Earth Ion-Host Lattice Interactions: 15. Analysis of the Spectra of Nd ³⁺ in Gd ₃ Sc ₂ Ga ₃ O ₁₂		5. TYPE OF REPORT & PERIOD COVERED Technical Report
		6. PERFORMING ORG. REPORT NUMBER
7. AUTHOR(s) Clyde A. Morrison Richard P. Leavitt Michael D. Gildner		8. CONTRACT OR GRANT NUMBER(s)
9. PERFORMING ORGANIZATION NAME AND ADDRESS Harry Diamond Laboratories 2800 Powder Mill Road Adelphi, MD 20783		10. PROGRAM ELEMENT, PROJECT, TASK AREA & WORK UNIT NUMBERS PRON: CJ32302101CJA9 DA: 1L161102A31B
11. CONTROLLING OFFICE NAME AND ADDRESS Night Vision and Electro-Optics Laboratory Ft. Belvoir, VA 22060		12. REPORT DATE May 1984
		13. NUMBER OF PAGES 25
14. MONITORING AGENCY NAME & ADDRESS (if different from Controlling Office)		15. SECURITY CLASS. (of this report) Unclassified
		15a. DECLASSIFICATION/DOWNGRADING SCHEDULE
16. DISTRIBUTION STATEMENT (of this Report) Approved for public release; distribution unlimited.		
17. DISTRIBUTION STATEMENT (of the abstract entered in Block 20, if different from Report)		
18. SUPPLEMENTARY NOTES DRCMS: 61110231B0011 HDL Project: 324332		
19. KEY WORDS (Continue on reverse side if necessary and identify by block number) Rare earth Mixed garnet Spectra Laser Judd-Ofelt Crystal-field parameters Neodymium Branching ratios		
20. ABSTRACT (Continue on reverse side if necessary and identify by block number) The Judd-Ofelt theory of induced electric-dipole transitions is used to calculate multiplet-to-multiplet line strengths, lifetimes, and branching ratios, and line-to-line squared matrix elements between all the energy levels considered for the triply ionized lanthanides Ce ³⁺ through Yb ³⁺ in Gd ₃ Sc ₂ Ga ₃ O ₁₂ . Magnetic-dipole transitions are also calculated. The even-n B _{nm} used in the calculations are obtained by smoothing the phenomenological B _{nm} obtained by fitting experimental data on neodymium. The odd-n A _{nm} are obtained from appropriate lattice sums. These results are compared with neodymium in several popular host materials. Detailed intensity		

DD FORM 1473
1 JAN 75

EDITION OF 1 NOV 65 IS OBSOLETE

1

UNCLASSIFIED

SECURITY CLASSIFICATION OF THIS PAGE (When Data Entered)

UNCLASSIFIED

SECURITY CLASSIFICATION OF THIS PAGE(When Data Entered)

20. ABSTRACT (Cont'd)

* calculations (line to line) and g-factor calculations have been performed and the results are attached in microfiche form.

Accession No.	
DTIC TAB	<input checked="checked" type="checkbox"/>
Unannounced	<input type="checkbox"/>
Justification	<input type="checkbox"/>
By	
Distribution/	
Availability Codes	
Avail	or
Dist	al
A-1	



CONTENTS

	<u>Page</u>
1. INTRODUCTION	5
2. CRYSTAL FIELD	6
3. SCANDIUM AND GALLIUM SITES	13
4. CONCLUSION	15
ACKNOWLEDGEMENT	15
LITERATURE CITED	16
APPENDIX A.--COMPUTER OUTPUT	19
DISTRIBUTION	23

FIGURE

1. Multiplet-to-multiplet fluorescence branching ratios for transitions originating at $^4F_{3/2}$ level for Nd^{3+} in various hosts 12

TABLES

1. Crystallographic Data for $Gd_3Sc_2Ga_3O_{12}$	6
2. Point-Charge, Point-Dipole, and Self-Induced Lattice Sums A_{nm} ($cm^{-1}/\text{\AA}^n$), for $Gd_3Sc_2Ga_3O_{12}$	7
3. Point-Charge Lattice Sums A_{nm} ($cm^{-1}/\text{\AA}^n$), for $Y_3Al_5O_{12}$ and $Y_3Ga_5O_{12}$..	7
4. Best Fit of Calculated Energy Levels to Experimental Energy Levels of $Nd:Gd_3Sc_2Ga_3O_{12}$ Using All Experimental Data of Kaminskii et al ...	8
5. Best fit of Calculated Energy Levels to Experimental Energy Levels of $Nd:Gd_3Sc_2Ga_3O_{12}$ with Level at 4000 cm^{-1} Removed from Experimental Data Given in Table 4	9
6. Best fit B_{nm} for Nd in $Gd_3Sc_2Ga_3O_{12}$ and Phenomenological A_{nm} ($A_{nm} = B_{nm}/\rho n(Nd)$)	10
7. Smoothed Crystal-Field Parameters B_{nm} (cm^{-1}) for All Rare-Earth Ions R^{3+} for $R:Gd_3Sc_2Ga_3O_{12}$	10
8. Calculated Judd-Ofelt Intensity Parameters for $R:Gd_3Sc_2Ga_3O_{12}$	11

TABLES (Cont'd)

	<u>Page</u>
9. Calculated Judd-Ofelt Intensity Parameters for $R:Y_3Al_5O_{12}$	11
10. Calculated Judd-Ofelt Intensity Parameters for $R:LiYF_4$	12
11. Distance to Nearest Oxygen Ions, R (Å), and Number of Oxygen Ions at that Distance for Metal Sites in $Gd_3Sc_2Ga_3O_{12}$	13
12. Ionic Radii (Å) and Coordination Numbers (CN) of Several Ions	13
13. Point-Charge Lattice Sums A_{nm} ($cm^{-1}/\text{\AA}^n$) for Sc^{3+} Site in $Gd_3Sc_2Ga_3O_{12}$	14
14. Point-Charge Lattice Sums A_{nm} ($cm^{-1}/\text{\AA}^n$), for Ga^{3+} Site in $Gd_3Sc_2Ga_3O_{12}$	14

1. INTRODUCTION

The material $\text{Gd}_3\text{Sc}_2\text{Ga}_3\text{O}_{12}$ is a mixed garnet with the same crystal structure as the popular laser material $\text{Y}_3\text{Al}_5\text{O}_{12}$ (YAG).^{1,2} The chemical formula for YAG is sometimes written as $\text{Y}_3\text{Al}_2\text{Al}_3\text{O}_{12}$ to illustrate that two types of aluminum sites exist in this material. In the material $\text{Gd}_3\text{Sc}_2\text{Ga}_3\text{O}_{12}$ each ion type occupies a single site type. The optical spectra and laser action of Nd^{3+} in $\text{Gd}_3\text{Sc}_2\text{Ga}_3\text{O}_{12}$ have been reported by Kaminskii.^{3,4} An interesting feature of this material is that if it is doped with both Nd^{3+} and Cr^{3+} , energy is transferred efficiently from the Cr^{3+} to the Nd^{3+} impurities.⁵ The microwave phonon attenuation of this and related garnets has been measured at a number of different temperatures.⁶ The indices of refraction of a number of related mixed rare-earth garnets⁷ have been measured in the wavelength region from 5200 to 6200 Å. Although the optical spectra of only one rare-earth ion in this host, Nd^{3+} , have been reported, we considered the host important enough to do a preliminary crystal-field analysis of rare-earth ions.

In this report we use techniques reported previously^{8,9} to obtain first estimates of the crystal-field parameters for $\text{Nd}:\text{Gd}_3\text{Sc}_2\text{Ga}_3\text{O}_{12}$. These parameters are used as starting values in a program that varies the crystal-field parameters to obtain a best least-squares fit to the experimental data. The resulting crystal-field parameters are used in conjunction with odd-fold lattice sums to obtain the Judd-Ofelt intensity parameters, the level-to-level line strengths for electric- and magnetic-dipole transitions, and the branching ratios for the entire rare-earth series. Comparisons to corresponding calculations on other host materials are made throughout.

¹M. J. Weber, *Handbook of Lasers*, Chemical Rubber Company, Cleveland, Ohio (1971), chapter 13, p 371.

²C. A. Morrison and R. P. Leavitt, *Spectroscopic Properties of Triply Ionized Lanthanides in Transparent Host Materials*, in *Handbook on the Physics and Chemistry of Rare Earths*, Vol 5, K. A. Gschneidner and L. Eyring, Jr., eds., North Holland, New York (1982), p 632.

³A. A. Kaminskii, Kh. S. Bagdasarov, G. A. Bogomolova, M. M. Gritsenko, A. M. Kevorkov, and S. E. Sarkisov, *Luminescence and Stimulated Emission of Nd^{3+} Ions in $\text{Gd}_3\text{Sc}_2\text{Ga}_3\text{O}_{12}$ Crystals*, *Phys. Stat. Sol. (a)* **34** (1976), K109.

⁴A. A. Kaminskii, *Laser Crystals*, Springer-Verlag, New York (1981), p 133.

⁵D. Pruss, G. Huber, A. Biemowski, V. V. Laptev, I. A. Shcherbakov, and Y. V. Zharikov, *Efficient Cr^{3+} Sensitized $\text{Nd}^{3+}:\text{GdScGa}$ --Garnet Laser at 1.06 μm* , *Appl. Phys.* **B28** (1982), 358. See also E. V. Zharikov, V. V. Laptev, E. I. Sidorova, Yu. P. Timefeev, and I. A. Shcherbakov, *Absolute Quantum Efficiency of the Luminescence of Cr^{3+} Ions in Gadolinium Gallium and Gadolinium Scandium Gallium Garnet Crystals*, *Sov. J. Quant. Electron.* **12** (1982), 1124.

⁶M. Dutoit, J. C. Walling, and D. S. Boudreaux, *Microwave Phonon Attenuation in Rare-Earth Garnets: Ion-Phonon Interactions*, *Phys. Rev.* **B11** (1975), 349.

⁷S. H. Wemple and W. J. Tabor, *Refractive Index Behavior of Garnets*, *J. Appl. Phys.* **44** (1973), 1395.

⁸C. A. Morrison and R. P. Leavitt, *Crystal Field Analysis of Triply Ionized Rare Earth Ions in Lanthanum Trifluoride*, *J. Chem. Phys.* **71** (1979), 2366.

⁹R. P. Leavitt and C. A. Morrison, *Crystal Field Analysis of Triply Ionized Rare Earth Ions in Lanthanum Trifluoride. II. Intensity Calculations*, *J. Chem. Phys.* **73** (1980), 749.

2. CRYSTAL FIELD

The crystallographic data¹⁰ on $\text{Gd}_3\text{Sc}_2\text{Ga}_3\text{O}_{12}$ are given in table 1. We were unable to find a refined x-ray study of this material and have taken the oxygen positions to be the same as reported for $\text{Y}_3\text{Ga}_5\text{O}_{12}$. The lattice sums, A_{nm} , were evaluated using these x-ray data. Effective charges, Z_i ($q_i = eZ_i$), in units of the magnitude of the electron charge, were taken as $Z_{\text{Gd}} = Z_{\text{Sc}} = 3$, $Z_{\text{Ga}} = 1$, and $Z_{\text{O}} = -1.5$. The resulting point-charge contributions to the A_{nm} are shown in column 2 of table 2. The point-dipole¹¹ and self-induced¹² contributions to the A_{nm} were also evaluated and are shown in columns 3 and 4. In the evaluation of these latter contributions, the polarizability of oxygen was taken to be one-tenth of the handbook value (based on previous experience). The point-charge contributions to the A_{nm} for the isostructural materials $\text{Y}_3\text{Al}_5\text{O}_{12}$ ¹³ and $\text{Y}_3\text{Ga}_5\text{O}_{12}$ ¹⁴ are included in table 3 for comparison.

TABLE 1. CRYSTALLOGRAPHIC DATA FOR $\text{Gd}_3\text{Sc}_2\text{Ga}_3\text{O}_{12}$
(CUBIC SPACE GROUP Ia3d, No. 230, Z = 8)^a

Ion	Position	Symmetry	x	y	z
Gd	24(c)	D ₂	0	1/4	1/8
Sc	16(a)	C _{3i}	0	0	0
Ga	24(d)	S ₄	3/8	0	1/4
O	96(h)	C ₁	-0.0272	0.0558	0.1501

^aFractional oxygen positions are from isostructural material $\text{Y}_3\text{Ga}_5\text{O}_{12}$ (Morrison and Leavitt, ref 2, p 643). Lattice constant is $a = 12.5668 \text{ \AA}$ (Brandle and Barns, ref 10).

¹⁰C. D. Brandle and R. L. Barns, *Crystal Stoichiometry and Growth of Rare-Earth Garnets Containing Scandium*, J. Cryst. Growth **20** (1979), 1.

¹¹C. A. Morrison, *Dipolar Contributions to the Crystal Field in Ionic Solids*, Solid State Commun. **18** (1976), 153.

¹²C. A. Morrison, G. F. de Sá, and R. P. Leavitt, *Self-Induced Multipole Contribution to the Single-Electron Crystal Field*, J. Chem. Phys. **76** (1982), 3899.

¹³D. E. Wortman, C. A. Morrison, and N. Karayianis, *Rare Earth Ion-Host Lattice Interactions: 11. Lanthanides in $\text{Y}_3\text{Al}_5\text{O}_{12}$* , Harry Diamond Laboratories, HDL-TR-1773 (August 1976).

¹⁴N. Karayianis, D. E. Wortman, and C. A. Morrison, *Rare Earth Ion-Host Lattice Interactions: 12. Lanthanides in $\text{Y}_3\text{Ga}_5\text{O}_{12}$* , Harry Diamond Laboratories, HDL-TR-1793 (July 1977).

TABLE 2. POINT-CHARGE, POINT-DIPOLE, AND SELF-INDUCED LATTICE SUMS A_{nm} ($\text{cm}^{-1}/\text{\AA}^n$), FOR $\text{Gd}_3\text{Sc}_2\text{Ga}_3\text{O}_{12}$

A_{nm}	Point-charge ^a	Point-dipole ^b	Self-induced ^b	Total
A_{20}	4616.	-1006.	-38.42	3572.
A_{22}	2294.	-1324.	39.44	1010.
A_{32}	i224.5	-i679.5	i51.47	-i403.6
A_{40}	224.1	-234.4	2.043	-8.190
A_{42}	-4142.	-56.08	208.6	-3990.
A_{44}	-2130.	-133.7	122.2	-2141.
A_{52}	-i1602.	-i19.33	i106.5	-i1515.
A_{54}	i979.0	i22.26	-i58.05	i943.2
A_{60}	-1036.	-26.88	82.22	-981.1
A_{62}	-406.6	17.89	38.58	-350.1
A_{64}	528.4	20.26	-44.30	504.4
A_{66}	-401.0	29.17	35.10	-336.8
A_{72}	i61.01	i4.051	-i7.057	i58.01
A_{74}	i150.1	i32.29	-i21.02	i161.4
A_{76}	-i151.5	-i8.299	i13.14	-i146.6

^aX-ray data are given in table 1. Effective charges are $Z_{\text{Gd}} = +3$, $Z_{\text{Sc}} = +3$, $Z_{\text{Ga}} = +1$, and $Z_{\text{O}} = -1.5$.

^bPolarizability of oxygen, α_{O} , is taken to be 0.244 \AA^3 .

TABLE 3. POINT-CHARGE LATTICE SUMS A_{nm} ($\text{cm}^{-1}/\text{\AA}^n$) FOR $\text{Y}_3\text{Al}_5\text{O}_{12}$ AND $\text{Y}_3\text{Ga}_5\text{O}_{12}$

A_{nm}	$\text{Y}_3\text{Al}_5\text{O}_{12}$ ^a	$\text{Y}_3\text{Ga}_5\text{O}_{12}$ ^b
A_{20}	1453	4948.
A_{22}	2292	2459.
A_{32}	-i2758	i246.2
A_{40}	-614.6	751.6
A_{42}	-4916	-4649.
A_{44}	-2799	-2390.
A_{52}	-i2015	-i1840.
A_{54}	i1159	i1125.
A_{60}	-1481	-1218.
A_{62}	-568.2	-477.9
A_{64}	546.2	621.1
A_{66}	-503.1	-471.4
A_{72}	i30.62	i73.38
A_{74}	i84.41	i180.6
A_{76}	-i176.2	-i182.2

^aX-ray data were taken from Morrison and Leavitt (ref 2, p 634). Effective charges are $Z_{\text{Y}} = +3$, $Z_{\text{Al}} = +1.92$, and $Z_{\text{O}} = -1.55$.

^bX-ray data were taken from Morrison and Leavitt (ref 2, p 643). Effective charges are $Z_{\text{Y}} = +3$, $Z_{\text{Ga}_1} = +3$, $Z_{\text{Ga}_2} = +1$, and $Z_{\text{O}} = -1.5$.

The A_{nm} of column 2 of table 2 were used to calculate crystal-field parameters B_{nm} for neodymium using

$$B_{nm} = \rho_n(\text{Nd})A_{nm} \quad (1)$$

where the $\rho_n(\text{Nd})$ are radial factors given in an earlier work.¹⁵ These B_{nm} were then used as initial values in a least-squares fit to the experimental data on $\text{Nd:Gd}_3\text{Sc}_2\text{Ga}_3\text{O}_{12}$. The best fit for all the reported data was extremely poor, and the resultant B_{nm} were far from those obtained for Nd^{3+} in the isostructural compounds $\text{Y}_3\text{Al}_5\text{O}_{12}$ and $\text{Y}_3\text{Ga}_5\text{O}_{12}$. These results are shown in table 4.

TABLE 4. BEST FIT OF CALCULATED ENERGY LEVELS TO EXPERIMENTAL ENERGY LEVELS OF $\text{Nd:Gd}_3\text{Sc}_2\text{Ga}_3\text{O}_{12}$ USING ALL EXPERIMENTAL DATA OF KAMINSKII ET AL (ref 3, 4) (E = experimental, T = theoretical)^a

Term		Prefix ^b	Energy (cm^{-1})							
$^4I_{9/2}$	E	-	0	107	168	263	763			
	T	-	-84	136	201	304	746			
$^4I_{11/2}$	E	1	978	010*	069	109	393	431		
	T	2	000	023	067	112	339	443		
$^4I_{13/2}$	E	3	907	920	000*	010	025	380	421	
	T	3	890	900	933	013*	192	337	406	
$^4I_{15/2}$	E	5	777	812	914	959	494*	510	557	
	T	5	772	812	915	009*	431	474	591	
	E	6	647							
	T	6	664							
$^4F_{3/2}$	E	11	434	499						
	T	11	434	494						

^aRms deviation is 45.95 cm^{-1} . Resulting $B_{nm} (\text{cm}^{-1})$ are $B_{20} = 187$, $B_{22} = -273$, $B_{40} = -390$, $B_{42} = -475$, $B_{44} = -2157$, $B_{60} = -2081$, $B_{62} = -307$, $B_{64} = 706$, and $B_{66} = -211$.

^bPrefix for entries to right. Asterisk indicates that, for that entry and succeeding entries in that row, prefix is increased by one. Thus for experimental data in $^4I_{11/2}$ we have

1 978 010* 069 ... = 1978 2010 2069 ...

¹⁵C. A. Morrison, N. Karayianis, and D. E. Wortman, Rare Earth Ion-Host Lattice Interactions: 4. Predicting Spectra and Intensities of Lanthanides in Crystals, Harry Diamond Laboratories, HDL-TR-1816 (June 1977).

For several reasons, we then chose to remove the level at 4000 cm^{-1} in an attempt to remedy the poor fit. First, our lattice-sum calculation predicts no line in the vicinity of the 4000- cm^{-1} line. Second, examination of the data on Nd^{3+} in other garnets² reveals at most four lines below 4200 cm^{-1} within the $^4\text{I}_{13/2}$ manifold. Third, Kaminskii et al³ mention extra lines in their data. Finally, and most importantly, rejection of the 4000- cm^{-1} line leads to a vastly improved fit of the data. The best fit to the experimental data (minus the 4000- cm^{-1} line) was obtained again; results of this fit are shown in table 5. The rms deviation between the calculated and experimental energy levels was very small ($\sim 2 \text{ cm}^{-1}$) and represents one of the best fits that we have ever obtained to experimental energy-level data in crystals. Shown in table 6 are the best-fit B_{nm} and the phenomenological A_{nm} (for even n) obtained from the best fit B_{nm} by

$$A_{nm} = B_{nm}/\rho_n(\text{Nd}) \quad , \quad (2)$$

where $\rho_n(\text{Nd})$ is the same as in equation (1).

TABLE 5. BEST FIT OF CALCULATED ENERGY LEVELS TO EXPERIMENTAL ENERGY LEVELS OF $\text{Nd}:\text{Gd}_3\text{Sc}_2\text{Ga}_3\text{O}_{12}$ WITH LEVEL AT 4000 cm^{-1} REMOVED FROM EXPERIMENTAL DATA GIVEN IN TABLE 4^a

Term		Prefix ^b	Energy (cm^{-1})							
$^4\text{I}_{9/2}$	E	-	0	107	168	263	763			
	T	-	-1	105	168	267	762			
$^4\text{I}_{11/2}$	E	1	978	010*	069	109	393	431		
	T	1	979	006*	070	107	394	435		
$^4\text{I}_{13/2}$	E	3	907	920	010*	025	-	380	421	
	T	3	911	923	009*	020	367	381	419	
$^4\text{I}_{15/2}$	E	5	777	812	914	959	494*	510	557	
	T		777	809	916	962	495*	512	557	
	E	6	647							
	T	6	643							
$^4\text{F}_{3/2}$	E	11	434	499						
	T	11	435	498						

^aRms is 2.37 cm^{-1} . Resulting best-fit B_{nm} are given in table 6.

^bFor explanation of notation, see footnotes of table 4.

²C. A. Morrison and R. P. Leavitt, *Spectroscopic Properties of Triply Ionized Lanthanides in Transparent Host Materials*, in *Handbook on the Physics and Chemistry of Rare Earths*, Vol 5, K. A. Gschneidner and L. Eyring, Jr., eds., North Holland, New York (1982), p 632.

³A. A. Kaminskii, Kh. S. Bagdasarov, G. A. Bogomolova, M. M. Gritsenko, A. M. Kevorkov, and S. E. Sarkisov, *Luminescence and Stimulated Emission of Nd^{3+} Ions in $\text{Gd}_3\text{Sc}_2\text{Ga}_3\text{O}_{12}$ Crystals*, *Phys. Stat. Sol. (a)* 34 (1976), K109.

TABLE 6. BEST FIT B_{nm} FOR Nd IN $Gd_3Sc_2Ga_3O_{12}$ AND
PHENOMENOLOGICAL A_{nm} ($A_{nm} = B_{nm}/\rho_n(Nd)$)

nm	$B_{nm} (cm^{-1})$	$A_{nm} (cm^{-1}/\text{\AA}^n)$
20	434	2544
22	90	529
40	-67	-115
42	-1818	-3148
44	-921	-1595
60	-1485	-934
62	-679	-427
64	771	485
66	-661	-416

The A_{nm} obtained by using equation (2), as given in table 6, were then compared to the various contributions to the A_{nm} given in table 2. It is apparent that if different polarizabilities and effective charges were chosen, the values of A_{nm} of table 2 could be brought into better agreement with those of table 6. However, because of the lack of refined x-ray data for $Gd_3Sc_2Ga_3O_{12}$ (that is, the oxygen positions are unknown), no attempt was made to investigate such changes. The phenomenological A_{nm} of table 6 for even n were used in equation (1) to obtain B_{nm} for the entire rare-earth series. These B_{nm} are given in table 7.

TABLE 7. SMOOTHED CRYSTAL-FIELD PARAMETERS $B_{nm} (cm^{-1})$ FOR ALL
RARE-EARTH IONS R^{3+} FOR $R:Gd_3Sc_2Ga_3O_{12}$

R	B_{20}	B_{22}	B_{40}	B_{42}	B_{44}	B_{60}	B_{62}	B_{64}	B_{66}
Ce	468	97.5	-86.8	-2372	-1202	-2187	-1000	1136	-974
Pr	447	93.0	-74.4	-2035	-1031	-1752	-801	910	-780
Nd	434	90.3	-66.5	-1818	-921	-1485	-679	771	-661
Pm	427	88.9	-61.5	-1680	-851	-1328	-607	690	-591
Sm	424	88.3	-58.1	-1589	-805	-1234	-564	641	-549
Eu	424	88.2	-55.7	-1522	-771	-1168	-534	606	-520
Gd	424	88.3	-53.6	-1465	-742	-1109	-507	576	-494
Th	426	88.6	-51.7	-1413	-716	-1049	-480	545	-467
Dy	428	89.0	-50.0	-1366	-692	-991	-453	515	-441
Ho	430	89.6	-48.6	-1327	-672	-945	-432	491	-421
Er	434	90.3	-47.5	-1299	-658	-918	-420	477	-409
Tm	438	91.2	-46.7	-1276	-646	-901	-412	468	-401
Yb	442	91.9	-45.3	-1239	-628	-852	-390	442	-379

The odd- n A_{nm} given in column 2 of table 2 were used to calculate the Judd-Ofelt intensity parameters, Ω_k , for all the rare-earth ions in $Gd_3Sc_2Ga_3O_{12}$. The Ω_k are given in table 8. In table 9 the corresponding Ω_k are calculated for $R:Y_3Al_5O_{12}$ and in table 10 the Ω_k are given for $R:LiYF_4$. The results in tables 9 and 10 are included here for comparison.

TABLE 8. CALCULATED JUDD-OFELT INTENSITY PARAMETERS
FOR $R:Gd_3Sc_2Ga_3O_{12}$ ^a

R	$\Omega_2 (10^{-20} \text{ cm}^2)$	$\Omega_4 (10^{-20} \text{ cm}^2)$	$\Omega_6 (10^{-20} \text{ cm}^2)$
Ce	12.75	2.817	26.21
Pr	7.136	1.423	11.19
Nd	6.880	0.8867	6.139
Pm	3.982	0.6923	4.717
Sm	3.472	0.5808	3.903
Eu	2.747	0.4554	2.764
Gd	2.150	0.3540	1.909
Tb	3.754	0.5356	4.615
Dy	2.761	0.3963	2.866
Ho	2.255	0.3210	2.093
Er	2.162	0.2998	1.974
Tm	2.103	0.2846	1.906
Yb	1.774	0.2360	1.452

^aOdd- n A_{nm} used in calculation of Ω_k are from column 2 of table 2.

TABLE 9. CALCULATED JUDD-OFELT INTENSITY PARAMETERS
FOR $R:Y_3Al_5O_{12}$ ^a

R	$\Omega_2 (10^{-20} \text{ cm}^2)$	$\Omega_4 (10^{-20} \text{ cm}^2)$	$\Omega_6 (10^{-20} \text{ cm}^2)$
Ce	1.933	8.751	39.78
Pr	1.082	4.413	16.96
Nd	1.043	2.855	9.293
Pm	0.6036	2.197	7.147
Sm	0.5264	1.871	5.864
Eu	0.4165	1.422	4.186
Gd	0.3259	1.065	2.887
Tb	0.5692	2.066	7.029
Dy	0.4186	1.422	4.360
Ho	0.3418	1.112	3.181
Er	0.3278	1.057	3.001
Tm	0.3188	1.023	2.899
Yb	0.2690	0.8288	2.208

^aOdd-fold A_{nm} used in calculation of Ω_k are from column 2 of table 3.

The odd A_{nm} of column 2 of table 2 were also used to calculate the line-to-line transition probabilities for electric-dipole and magnetic-dipole transitions for all the rare-earth ions, R^{3+} , in $R:Gd_3Sc_2Ga_3O_{12}$. Also, the branching ratios and g-factors were calculated. These results are included in the form of microfiche copies of computer outputs, at the end of the report; these computer outputs are explained in appendix A. The branching ratios for $^4F_{3/2}$ to 4I_J for $J = 15/2, 13/2, 11/2$, and $9/2$ are shown in figure 1 for Nd^{3+} in $Y_3Al_5O_{12}$ (YAG), $LiYF_4$ (YLF), and $Gd_3Sc_2Ga_3O_{12}$. Results for Nd^{3+} in YAG and YLF are included because experimental data are available for these host materials. It is apparent that the calculated results agree well with the experimental results; this gives further confidence in the accuracy of the calculations on $Gd_3Sc_2Ga_3O_{12}$. Thus, if the x-ray positions assumed for $Gd_3Sc_2Ga_3O_{12}$ are a good approximation, we should expect the results shown in figure 1 for Nd^{3+} in this host to be quite accurate.

TABLE 10. CALCULATED JUDD-OFELT INTENSITY PARAMETERS
FOR R:LiYF₄^a

R	$\Omega_2 (10^{-20} \text{ cm}^2)$	$\Omega_4 (10^{-20} \text{ cm}^2)$	$\Omega_6 (10^{-20} \text{ cm}^2)$
Ce	22.28	6.161	52.72
Pr	12.47	3.111	22.48
Nd	12.02	1.949	12.33
Pm	6.956	1.519	9.476
Sm	6.066	1.277	7.845
Eu	4.799	0.9967	5.551
Gd	3.755	0.7706	3.830
Tb	6.559	1.213	9.304
Dy	4.824	0.8864	5.773
Ho	3.939	0.7139	4.213
Er	3.777	0.6686	3.975
Tm	3.673	0.6367	3.839
Yb	3.100	0.5260	2.924

^aEven- n $B_{\Omega m}$ are from D. E. Wortman, N. Karayianis, and C. A. Morrison, Rare Earth Ion-Host Lattice Interactions: 6. Lanthanides in LiYF₄, Harry Diamond Laboratories, HDL-TR-1770 (August 1976). Odd- n $A_{\Omega m}$ are from L. Esterowitz, F. J. Bartoli, R. E. Allen, D. E. Wortman, C. A. Morrison, and R. P. Leavitt, Energy Levels and Line Intensities of Pr³⁺ in LiYF₄, Phys. Rev. B19 (1979), 6442.

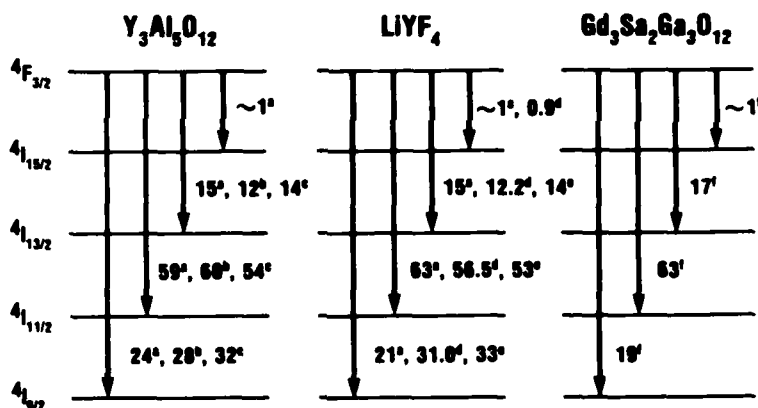


Figure 1. Multiplet-to-multiplet fluorescence branching ratios (in percent) for transitions originating at the $4F_{3/2}$ level for Nd³⁺ in various hosts:

- calculated, K. K. Deb, R. G. Buser, C. A. Morrison, and R. P. Leavitt, Crystal Fields and Intensities of Triply Ionized Rare-Earth Ions in Cubic Lanthanum Oxyfluoride: An Efficient $4F_{3/2} \rightarrow 4I_{9/2}$ LaOF:Nd Laser, J. Opt. Soc. Am. 71 (1981), 1463;
- experimental, R. K. Watts, Jr., Branching Ratios for YAlG:Nd³⁺, J. Opt. Soc. Am. 61 (1971), 123;
- experimental, S. Singh, R. G. Smith, and L. G. Van Uitert, Stimulated Emission Cross Section and Fluorescent Quantum Efficiency of Nd³⁺ in Yttrium Garnet at Room Temperature, Phys. Rev. B10 (1974), 2566;
- experimental, H. P. Jenssen, Center for Materials Science and Engineering and Department of Electrical Engineering, Massachusetts Institute of Technology, Cambridge, MA 02139 (personal communication);
- experimental, T. L. Lomheim and L. G. DeShazer, New Procedure of Determining Neodymium Fluorescence Branching Ratios as Applied to 25 Crystals and Glass Hosts, Opt. Commun. 24 (1978), 89;
- calculated, this work.

3. SCANDIUM AND GALLIUM SITES

To investigate the possibility of other site occupancy by Nd^{3+} or other ions in $\text{Gd}_3\text{Sc}_2\text{Ga}_3\text{O}_{12}$, the distances between ions and the number of ion pairs at a given distance were calculated for all the sites in this compound. The results are given in table 11. The ionic radii of several ions in different coordination are given in table 12. The coordination number (CN), the number of nearest ions, for the Gd site is assumed to be 8, since the two groups of oxygen are nearly the same (see table 11) and the next set of ions is much further away (~ 3.14 Å). The ionic radii of Nd^{3+} and Gd^{3+} for CN = 8 are nearly the same, so we should expect the Nd^{3+} to predominantly enter the Gd^{3+} site in $\text{Gd}_3\text{Sc}_2\text{Ga}_3\text{O}_{12}$. However, it is possible that some of the Nd^{3+} may enter the Sc^{3+} site in this compound. For this reason, the point-charge lattice sums A_{nm} were calculated for the Sc^{3+} site in $\text{Gd}_3\text{Sc}_2\text{Ga}_3\text{O}_{12}$; the results are given in table 13. Also included in table 13 are the B_{nm} for Nd^{3+} calculated using equation (1). In these calculations, the effective charges on the ions are the same as used in the calculation of table 2. The crystal-field parameters, B_{nm} , for Nd^{3+} in the scandium site as given in table 13 are unrealistically large. This possibly is due to the inaccuracies in the x-ray data. No further calculation was done using the B_{nm} for the scandium site.

TABLE 11. DISTANCE TO NEAREST OXYGEN IONS,
R (Å), AND NUMBER OF OXYGEN IONS AT THAT DISTANCE FOR METAL
SITES IN $\text{Gd}_3\text{Sc}_2\text{Ga}_3\text{O}_{12}$ ^a

Site	R	Number	R	Number
Gd	2.39	4	2.48	4
Sc	2.04	6	-	-
Ga	1.99	4	-	-

^aX-ray data used are given in table 1.

TABLE 12. IONIC RADII (Å) AND COORDINATION NUMBERS (CN) OF
SEVERAL IONS^a

Ion	Ionic radius	CN
Gd^{3+}	1.06	8
Nd^{3+}	1.12	8
Sc^{3+}	.87	6
Ga^{3+}	.47	4
Cr^{3+}	.615	6 ^b

^aR. D. Shannon and C. J. Prewitt, *Effective Ionic Radii in Oxides and Fluorides*, Acta. Cryst. B25 (1969), 925. Ionic radius is based on oxygen ion in 6 coordination having value 1.40 Å.

^bIonic radius of Cr^{3+} in 4 coordination is not given in above reference.

TABLE 13. POINT-CHARGE LATTICE SUMS A_{nm} ($\text{cm}^{-1}/\text{\AA}^n$) FOR Sc^{3+} SITE IN $\text{Gd}_3\text{Sc}_2\text{Ga}_3\text{O}_{12}$

nm	A_{nm}^a	$B_{nm}(\text{Nd})^b$
20	812	139
40	-11413	-6592
43	13327	7698
60	666	1058
R 63	2099	3336
I 63	52	83
R 66	687	1092
I 66	25	39

^aX-ray data used are given in table 1. Effective charges on ions are as in table 2. Lattice sum was performed for Sc^{3+} site at (0,0,0), and a rotation was performed so that C_{3i} axis is along a body diagonal. Euler angles used are $\alpha = -45^\circ$, $\beta = -54.736^\circ$, and $\gamma = 28.319^\circ$. $bB_{nm}(\text{Nd})$ are calculated using equation (1).

The point-charge lattice sums were calculated for the Ga site (S_4 symmetry) in $\text{Gd}_3\text{Sc}_2\text{Ga}_3\text{O}_{12}$; the results are given in table 14. It is highly unlikely that the Nd^{3+} enters this site, because of the large mismatch in ionic radii as given in table 12. However it is quite possible that Cr^{3+} doped in this crystal, as reported elsewhere,⁵ may enter this site or perhaps the Sc^{3+} site (see table 12). If the Cr^{3+} were to enter the Ga site substitutionally, the absorption should be quite intense because of the odd-n A_{nm} present in S_4 symmetry. Thus it would be possible to easily pump the Cr^{3+} ion and observe the transfer from Cr^{3+} to a substitutional rare-earth impurity in $\text{Gd}_3\text{Sc}_2\text{Ga}_3\text{O}_{12}$. In future work, we expect to use the results in table 14 to estimate the splittings of levels of Cr^{3+} in this host.

TABLE 14. POINT-CHARGE LATTICE SUMS A_{nm} ($\text{cm}^{-1}/\text{\AA}^n$) FOR Ga^{3+} SITE IN $\text{Gd}_3\text{Sc}_2\text{Ga}_3\text{O}_{12}$

nm	A_{nm}^a
20	739
R 32	24281
I 32	-608
40	-13749
44	5515
R 5	2882
I 52	-67
60	-88
R 64	3459
I 64	-285
R 72	-1364
I 72	48
R 76	956
I 76	-121

^aX-ray data used are given in table 1. Effective charges on ions are as in table 2. Lattice sum was performed for Ga^{3+} site at (0,0,0), and a rotation was performed so that S_4 axis is along z axis. Euler angles used are $\alpha = 0^\circ$, $\beta = 90^\circ$, and $\gamma = 59.5628^\circ$.

⁵D. Pruss, G. Huber, A. Biemowski, V. V. Laptev, I. A. Shcherbakov, and Y. V. Zharikov, Efficient Cr^{3+} Sensitized $\text{Nd}^{3+}:\text{GdScGa--Garnet}$ Laser at 1.06 μm , *Appl. Phys. B28* (1982), 358. See also E. V. Zharikov, V. V. Laptev, E. I. Sidorova, Yu. P. Timefeev, and I. A. Shcherbakov, Absolute Quantum Efficiency of the Luminescence of Cr^{3+} Ions in Gadolinium Gallium and Gadolinium Scandium Gallium Garnet Crystals, *Sov. J. Quant. Electron.* 12 (1982), 1124.

4. CONCLUSION

We have analyzed the experimental spectra of Nd^{3+} in the host $\text{Gd}_3\text{Sc}_2\text{Ga}_3\text{O}_{12}$. By omitting one of the reported energy levels we were able to obtain an excellent fit ($\text{rms} \approx 2 \text{ cm}^{-1}$) to the experimental data. The resulting phenomenological crystal-field parameters, B_{nm} , were used to obtain B_{nm} for the entire rare-earth series.⁸ Point-charge lattice sums A_{nm} were calculated for effective charges of $Z_{\text{O}} = -1.5$, $Z_{\text{Ga}} = +1$, $Z_{\text{Sc}} = +3$, and $Z_{\text{Gd}} = +3$. The even- n B_{nm} calculated as in earlier work² agreed quite reasonably with the phenomenological B_{nm} obtained by fitting the experimental data. The odd- n A_{nm} from the point-charge lattice sums were used along with the phenomenological B_{nm} to calculate the crystal-field-split energy levels, transition intensities, branching ratios, g values, and lifetimes for the low-lying energy levels of all the rare-earth ions in the Gd^{3+} sites in $\text{Gd}_3\text{Sc}_2\text{Ga}_3\text{O}_{12}$. The resulting branching ratios for Nd^{3+} and several other computed quantities were compared with standard laser-host materials (YAG, YLF) with few striking differences. The laser advantages of the garnet $\text{Gd}_3\text{Sc}_2\text{Ga}_3\text{O}_{12}$ appear to lie in the fact that the material can be easily doped with transition elements such as Cr^{3+} and still produce high-optical-quality crystals.

Acknowledgement

We wish to thank Jeffrey Paul of NVEOL for suggesting an analysis of the spectra of rare-earth ions in this material and for providing financial support.

²C. A. Morrison and R. P. Leavitt, *Spectroscopic Properties of Triply Ionized Lanthanides in Transparent Host Materials*, in *Handbook on the Physics and Chemistry of Rare Earths*, Vol 5, K. A. Gschneidner and L. Eyring, Jr., eds., North Holland, New York (1982), p 632.

⁸C. A. Morrison and R. P. Leavitt, *Crystal Field Analysis of Triply Ionized Rare Earth Ions in Lanthanum Trifluoride*, *J. Chem. Phys.* 71 (1979), 2366.

LITERATURE CITED

- (1) M. J. Weber, Handbook of Lasers, Chemical Rubber Company, Cleveland, Ohio (1971), chapter 13, p 371.
- (2) C. A. Morrison and R. P. Leavitt, Spectroscopic Properties of Triply Ionized Lanthanides in Transparent Host Materials, in Handbook on the Physics and Chemistry of Rare Earths, Vol 5, K. A. Gschneidner and L. Eyring, Jr., eds., North Holland, New York (1982), p 632.
- (3) A. A. Kaminskii, Kh. S. Bagdasarov, G. A. Bogomolova, M. M. Gritsenko, A. M. Kevorkov, and S. E. Sarkisov, Luminescence and Stimulated Emission of Nd^{3+} Ions in $\text{Gd}_3\text{Sc}_2\text{Ga}_3\text{O}_{12}$ Crystals, Phys. Stat. Sol. (a) 34 (1976), K109.
- (4) A. A. Kaminskii, Laser Crystals, Springer-Verlag, New York (1981), p 133.
- (5) D. Pruss, G. Huber, A. Biemowski, V. V. Laptev, I. A. Shcherbakov, and Y. V. Zharikov, Efficient Cr^{3+} Sensitized $\text{Nd}^{3+}:\text{GdScGa}$ --Garnet Laser at 1.06 μm , Appl. Phys. B28 (1982), 358. See also E. V. Zharikov, V. V. Laptev, E. I. Sidorova, Yu. P. Timefeev, and I. A. Shcherbakov, Absolute Quantum Efficiency of the Luminescence of Cr^{3+} Ions in Gadolinium Gallium and Gadolinium Scandium Gallium Garnet Crystals, Sov. J. Quant. Electron. 12 (1982), 1124.
- (6) M. Dutoit, J. C. Walling, and D. S. Boudreaux, Microwave Phonon Attenuation in Rare-Earth Garnets: Ion-Phonon Interactions, Phys. Rev. B11 (1975), 349.
- (7) S. H. Wemple and W. J. Tabor, Refractive Index Behavior of Garnets, J. Appl. Phys. 44 (1973), 1395.
- (8) C. A. Morrison and R. P. Leavitt, Crystal Field Analysis of Triply Ionized Rare Earth Ions in Lanthanum Trifluoride, J. Chem. Phys. 71 (1979), 2366.
- (9) R. P. Leavitt and C. A. Morrison, Crystal Field Analysis of Triply Ionized Rare Earth Ions in Lanthanum Trifluoride. II. Intensity Calculations, J. Chem. Phys. 73 (1980), 749.
- (10) C. D. Brandle and R. L. Barns, Crystal Stoichiometry and Growth of Rare-Earth Garnets Containing Scandium, J. Cryst. Growth 20 (1979), 1.
- (11) C. A. Morrison, Dipolar Contributions to the Crystal Field in Ionic Solids, Solid State Commun. 18 (1976), 153.
- (12) C. A. Morrison, G. F. de Sá, and R. P. Leavitt, Self-Induced Multipole Contribution to the Single-Electron Crystal Field, J. Chem. Phys. 76 (1982), 3899.

LITERATURE CITED (Cont'd)

- (13) D. E. Wortman, C. A. Morrison, and N. Karayianis, Rare Earth Ion-Host Lattice Interactions: 11. Lanthanides in $Y_3Al_5O_{12}$, Harry Diamond Laboratories, HDL-TR-1773 (August 1976).
- (14) N. Karayianis, D. E. Wortman, and C. A. Morrison, Rare Earth Ion-Host Lattice Interactions: 12. Lanthanides in $Y_3Ga_5O_{12}$, Harry Diamond Laboratories, HDL-TR-1793 (July 1977).
- (15) C. A. Morrison, N. Karayianis, and D. E. Wortman, Rare Earth Ion-Host Lattice Interactions: 4. Predicting Spectra and Intensities of Lanthanides in Crystals, Harry Diamond Laboratories, HDL-TR-1816 (June 1977).

APPENDIX A.--COMPUTER OUTPUT

Detailed intensity (line-to-line) and g-factor calculations have been performed, and the results are attached in the form of microfiche copies of computer printouts for each ion in the lanthanide series, from Ce^{3+} to Yb^{3+} . In this appendix, we describe the contents of the computer printouts and present excerpts from them.

The computer printout for each ion presents the following information, in sequence, as follows:

(1) even-k crystal-field parameters, centroid parameters, and crystal-field-split energy levels;

(2) approximate Judd-Ofelt intensity calculations (no J mixing) including the Judd-Ofelt parameters, multiplet-to-multiplet line strengths, lifetimes, and branching ratios;

(3) full Judd-Ofelt squared matrix elements for π (E parallel to D_2 axis) and σ (E perpendicular to D_2 axis) between all crystal-field-split levels;

(4) a summary of the full Judd-Ofelt calculations (J mixing included), including multiplet-to-multiplet line strengths, lifetimes, and branching ratios;

(5) approximate magnetic-dipole intensity calculations (no J mixing), including multiplet-to-multiplet line strengths, lifetimes, and branching ratios;

(6) full magnetic-dipole squared matrix elements for σ (B parallel to D_2 axis) and π (B perpendicular to D_2 axis) between all crystal-field-split levels;

(7) a summary of the full magnetic-dipole calculations (J mixing included), including multiplet-to-multiplet line strengths, lifetimes, and branching ratios; and

(8) g factors (for an odd number of f electrons).

An excerpt of the energy level table for Pr^{3+} is given in table A-1. The crystal-field-split levels are numbered in sequence, beginning with the ground state (these sequence numbers are used later as identifiers in the line-to-line intensity calculations). The "PCT. PURE" column gives an indication of the amount of J mixing by the crystal field. The crystal quantum number column ("2MU") identifies, for an even number of f electrons, the irreducible representation of C_2 to which a level belongs; levels with $2\mu = 0$ are Γ_1 and levels with $2\mu = 2$ are Γ_2 . For an odd number of electrons, all levels are

APPENDIX A

Kramers doublets with $2\mu = 1$ ($\Gamma_{3,4}$). The theoretical energy levels ("THEOR. ENERGY") correspond to those obtained using aqueous free-ion parameters.¹ (The "EXP. ENERGY" column is not relevant to this discussion.)

TABLE A-1. SAMPLE OF ENERGY LEVELS TABLE FROM
COMPUTER OUTPUT FOR Pr^{3+} IN $\text{Gd}_3\text{Sc}_2\text{Ga}_3\text{O}_{12}$

FREE ION	PCT PURE	2MU	THEOR. ENERGY	EXP. ENERGY
1 3H 4	99.9	0	0.0	0.0
2 3H 4	99.8	0	38.4	0.0
3 3H 4	99.6	2	44.8	0.0
4 3H 4	98.5	0	452.8	0.0
5 3H 4	96.1	0	474.6	0.0
6 3H 4	95.8	2	507.4	0.0
7 3H 4	95.7	2	516.4	0.0
8 3H 4	94.4	2	717.2	0.0
9 3H 4	94.6	0	731.2	0.0
64 1D 2	99.9	2	16733.5	0.0
65 1D 2	99.9	0	16746.3	0.0
66 1D 2	99.9	0	17273.2	0.0
67 1D 2	99.9	0	17438.5	0.0
68 1D 2	99.8	2	17458.4	0.0

A sample of the computer printout for the approximate Judd-Ofelt calculations for Pr^{3+} is given in table A-2. In the table, the upper right elements give the multiplet-to-multiplet line strengths in units of square angstroms. Thus, for instance, the total line strength for the $^3\text{H}_5 \rightarrow ^3\text{F}_3$ transition is $5.0 \times 10^{-5} \text{ \AA}^2$. The lower left elements in the table give the branching ratios for spontaneous emission, assuming that all levels within a multiplet are equally populated. The branching ratios, for example, for emission from the $^1\text{D}_2$ level are as follows:

0.06 for $^1\text{D}_2 \rightarrow ^3\text{F}_4$,
0.0069 for $^1\text{D}_2 \rightarrow ^3\text{F}_3$,
0.049 for $^1\text{D}_2 \rightarrow ^3\text{F}_2$,
0.081 for $^1\text{D}_2 \rightarrow ^3\text{H}_6$,
0.0063 for $^1\text{D}_2 \rightarrow ^3\text{H}_5$, and
0.72 for $^1\text{D}_2 \rightarrow ^3\text{H}_4$.

For a given initial state, all the branching ratios add up to unity. The calculation of the branching ratios neglects the dependence of the index of

¹W. T. Carnall, P. R. Fields, and K. Rajnak, *Electronic Levels in the Trivalent Lanthanide Aquo Ions. Pr^{3+} , Nd^{3+} , Sm^{3+} , Dy^{3+} , Ho^{3+} , Er^{3+} , and Tm^{3+}* , J. Chem. Phys. 49 (1968), 4412.

APPENDIX A

refraction on frequency. The diagonal elements in the table give the lifetimes of the excited multiplets, again assuming equal populations of the initial sublevels. The quoted lifetimes are in seconds and should be divided by $n(n^2 + 2)^2/9$, where n is the index of refraction.

TABLE A-2. SAMPLE OF COMPUTER PRINTOUT SUMMARY OF ELECTRIC-DIPOLE TRANSITION PROBABILITY CALCULATIONS FOR Pr^{3+} IN $\text{Gd}_3\text{Sc}_2\text{Ga}_3\text{O}_{12}$ USING APPROXIMATE JUDD-OFELT THEORY

	3H 4	3H 5	3H 6	3F 2	3F 3	3F 4	1G 4	1D 2
3H 4	0.0	7.1E-04	1.6E-04	1.9E-04	8.3E-04	5.5E-04	3.1E-05	6.1E-05
3H 5	1.0E+00	2.1E-01	7.5E-04	7.8E-04	5.0E-05	5.3E-04	4.9E-04	8.1E-07
3H 6	6.3E-01	3.7E-01	8.9E-02	3.4E-04	9.9E-04	6.0E-04	3.2E-04	1.7E-05
3F 2	5.7E-01	4.3E-01	2.8E-03	1.7E-02	7.3E-06	1.0E-04	9.9E-06	1.2E-05
3F 3	9.5E-01	1.6E-02	3.6E-02	7.3E-05	4.4E-03	1.6E-05	5.9E-05	2.4E-06
3F 4	7.4E-01	2.2E-01	3.8E-02	2.3E-03	6.4E-06	5.4E-03	4.2E-04	2.4E-05
1G 4	9.3E-02	7.0E-01	1.6E-01	3.4E-03	7.7E-03	3.6E-02	4.1E-03	9.2E-05
1D 2	7.2E-01	6.3E-03	8.1E-02	4.9E-02	6.9E-03	6.0E-02	7.9E-02	1.8E-03

An excerpt from the squared matrix-element table is given in table A-3 for the π -spectrum, $^3\text{H}_4 \rightarrow ^1\text{D}_2$ line-to-line electric-dipole transitions. It should be kept in mind that the polarizations referred to in this and the following table are with respect to the individual C_2 axes of the sites, and not the c -axis of the crystal. In table A-3, one number is presented for each transition, the squared matrix element p_z^2 of the z component of the electric dipole operator, in units of square angstroms.

TABLE A-3. EXCERPTS FROM COMPUTER OUTPUT FOR $\text{Pr}^{3+}:\text{Gd}_3\text{Sc}_2\text{Ga}_3\text{O}_{12}$ LINE-TO-LINE π ELECTRIC-DIPOLE TRANSITION PROBABILITY TABLE, FOR $^3\text{H}_4 \rightarrow ^1\text{D}_2$ TRANSITIONS WITH $2\mu = 0 \rightarrow 2\mu = 0$ AND $2\mu = 2 \rightarrow 2\mu = 2$

$2\mu = 0 \rightarrow 2\mu = 0$			
		65	6667
		1D 2	1D 21D 2
1 3H 4	3.568E-07	5.986E-06	8.124E-19
2 3H 4	1.921E-18	6.741E-18	6.936E-08
4 3H 4	8.742E-19	3.210E-20	6.083E-07
5 3H 4	3.344E-08	5.293E-07	6.175E-19
9 3H 4	3.136E-18	1.374E-18	4.265E-06
$2\mu = 2 \rightarrow 2\mu = 2$			
		64	68
		1D 2	1D 2
3 3H 4	6.741E-06	1.608E-19	
6 3H 4	4.875E-07	3.644E-18	
7 3H 4	1.652E-17	8.572E-08	
8 3H 4	2.502E-21	2.134E-06	

APPENDIX A

Table A-4 shows excerpts from the squared matrix elements table for the σ -spectrum, $^3H_4 + ^1D_2$ electric-dipole transitions. Again, the polarization (σ) is with respect to the site D_2 axis. For each transition, three numbers are presented in the table: $P_{xy}^2(\max)$, $P_{xy}^2(\min)$, and θ_m .

TABLE A-4. EXCERPTS FROM COMPUTER OUTPUT FOR $Pr^{3+}:Gd_3Sc_2Ga_3O_{12}$
LINE-TO-LINE σ ELECTRIC-DIPOLE TRANSITION PROBABILITY TABLE, FOR
 $^3H_4 + ^1D_2$ TRANSITIONS WITH $2\mu = 0 + 2\mu = 2$ AND $2\mu = 2 + 2\mu = 0$

$2\mu = 0 + 2\mu = 2$					
	1 3H 4	2 3H 4	4 3H 4	5 3H 4	9 3H 4
64 1D 2	4.686E-06 0.0 0.0	2.211E-07 0.0 0.0	3.440E-09 0.0 0.0	1.146E-06 0.0 0.0	6.598E-08 0.0 0.0
68 1D 2	3.062E-06 4.547E-13 90.0	1.140E-07 0.0 90.0	5.466E-07 5.684E-14 0.0	2.875E-07 2.842E-14 90.0	3.126E-06 0.0 0.0
$2\mu = 2 + 2\mu = 0$					
	65 1D 2	66 1D 2	67 1D 2		
3 3H 4	2.772E-07 2.842E-14 0.0	5.163E-06 4.547E-13 0.0	3.299E-06 4.547E-13 90.00		
6 3H 4	1.993E-09 1.110E-16 0.0	9.950E-08 0.0 0.0	1.874E-07 -2.842E-14 90.00		
7 3H 4	4.879E-07 8.527E-14 90.00	3.618E-06 0.0 90.00	1.553E-06 0.0 0.0		
8 3H 4	2.593E-06 0.0 90.00	5.663E-07 2.842E-14 90.00	2.482E-07 2.842E-14 0.0		

The remaining computer printout for intensity calculations consists of multiplet-to-multiplet tables and line-to-line tables, as described above. These tables have the same format as those already described. It should be remembered that, for the magnetic-dipole tables, π and σ are reversed; that is, σ corresponds to the B vector along z, and π corresponds to the B vector perpendicular to z. Also, for the magnetic-dipole transitions, the radiative lifetime is to be divided by n^3 , where n is the index of refraction.

For an odd number of electrons, all the levels are Kramers doublets, and g factors have been computed. The g tensor can be characterized by four numbers: $g_{||}$ (B parallel to z), $g_{\perp 1}$ and $g_{\perp 2}$ (maximum and minimum values of g_{\perp} for B in the x-y plane, respectively), and θ_m (the angle in the x-y plane for which g_{\perp} is a maximum). These are presented on the last page of the computer output.

DISTRIBUTION

ADMINISTRATOR
DEFENSE TECHNICAL INFORMATION CENTER
ATTN DTIC-DDA (12 COPIES)
CAMERON STATION, BUILDING 5
ALEXANDRIA, VA 22314

DIRECTOR
NIGHT VISION & ELECTRO-OPTICS LABORATORY
ATTN TECHNICAL LIBRARY
ATTN DR. R. BUSER
ATTN DR. A. PINTO
ATTN J. PAUL
ATTN J. HABERSAT
FT BELVOIR, VA 22060

DIRECTOR
DEFENSE ADVANCED RESEARCH
PROJECTS AGENCY
ATTN DR. J. FRIEBELE
1400 WILSON BLVD
ARLINGTON, VA 22209

DIRECTOR
DEFENSE NUCLEAR AGENCY
ATTN TECH LIBRARY
WASHINGTON, DC 20305

UNDER SECRETARY OF DEFENSE RES
& ENGINEERING
ATTN TECHNICAL LIBRARY, 3C128
WASHINGTON, DC 20301

OFFICE OF THE DEPUTY CHIEF OF STAFF,
FOR RESEARCH, DEVELOPMENT,
& ACQUISITION
DEPARTMENT OF THE ARMY
ATTN DAMA-ARZ-A, CHIEF SCIENTIST,
DR. RICHARD B. LEWIS
ATTN DAMA-ARZ-B, DR. I. R. HERSHNER
WASHINGTON, DC 20310

COMMANDER
US ARMY ARMAMENT MUNITIONS &
CHEMICAL COMMAND (AMCCOM)
US ARMY ARMAMENT RESEARCH &
DEVELOPMENT CENTER
ATTN DRDAR-TSS, STINFO DIV
DOVER, NJ 07801

COMMANDER
ATMOSPHERIC SCIENCES LABORATORY
ATTN TECHNICAL LIBRARY
WHITE SANDS MISSILE RANGE, NM 88002

DIRECTOR
US ARMY BALLISTIC RESEARCH LABORATORY
ATTN DRDAR-TSB-S (STINFO)
ABERDEEN PROVING GROUND, MD 21005

DIRECTOR
US ARMY ELECTRONICS WARFARE LABORATORY
ATTN J. CHARLTON
ATTN DELET-DD
FT MONMOUTH, NJ 07703

COMMANDING OFFICER
USA FOREIGN SCIENCE & TECHNOLOGY CENTER
FEDERAL OFFICE BUILDING
ATTN DRXST-BS, BASIC SCIENCE DIV
CHARLOTTESVILLE, VA 22901

COMMANDER
US ARMY MATERIALS & MECHANICS
RESEARCH CENTER
ATTN DRXMR-TL, TECH LIBRARY
WATERTOWN, MA 02172

US ARMY MATERIEL DEVELOPMENT
& READINESS COMMAND
5001 EISENHOWER AVE
ALEXANDRIA, VA 22333

US ARMY MATERIEL SYSTEMS ANALYSIS
ACTIVITY
ATTN DRXSY-MP (LIBRARY)
ABERDEEN PROVING GROUND, MD 21005

COMMANDER
US ARMY MISSILE & MUNITIONS
CENTER & SCHOOL
ATTN ATSK-CTD-F
ATTN DRDMI-TB, REDSTONE SCI INFO CENTER
REDSTONE ARSENAL, AL 35809

COMMANDER
US ARMY RESEARCH OFFICE (DURHAM)
PO BOX 12211
ATTN DR. ROBERT J. LONTZ
ATTN DR. B. D. GUENTHER
ATTN DR. CHARLES BOGOSIAN
RESEARCH TRIANGLE PARK, NC 27709

COMMANDER
USA RSCH & STD GP (EUR)
ATTN CHIEF, PHYSICS & MATH BRANCH
FPO NEW YORK 09510

COMMANDER
US ARMY TEST & EVALUATION COMMAND
ATTN DR. D. H. SLINNEY
ATTN TECH LIBRARY
ABERDEEN PROVING GROUND, MD 21005

COMMANDER
US ARMY TROOP SUPPORT COMMAND
ATTN DRXRES-RTL, TECH LIBRARY
NATICK, MA 01762

DISTRIBUTION (Cont'd)

COMMANDER
ATTN DRSEL-WL-MS, ROBERT NELSON
WHITE SANDS MISSILE RANGE, NM 88002

OFFICE OF NAVAL RESEARCH
ATTN DR. V. O. NICOLAI
ARLINGTON, VA 22217

DIRECTOR
NAVAL RESEARCH LABORATORY
ATTN CODE 2620, TECH LIBRARY BR
ATTN CODE 5554, DR F. BARTOLI
ATTN DR. L. ESTEROWITZ
ATTN CODE 5554, R. E. ALLEN
WASHINGTON, DC 20375

HQ, USAF/SAMI
WASHINGTON, DC 20330

DEPARTMENT OF COMMERCE
NATIONAL BUREAU OF STANDARDS
ATTN LIBRARY
ATTN H. S. PARKER
WASHINGTON, DC 20234

DIRECTOR
ADVISORY GROUP ON ELECTRON DEVICES
ATTN SECTRY, WORKING GROUP D
201 VARICK STREET
NEW YORK, NY 10013

AEROSPACE CORPORATION
PO BOX 92957
ATTN DR. M. BIRNBAUM
ATTN DR. N. C. CHANG
LOS ANGELES, CA 90009

ALLIED
ADVANCED APPLICATION DEPT
ATTN DR. A. BUDGOR
31717 LA TIEMDA DRIVE
WESTLAKE VILLAGE, CA 91362

AMES LABORATORY DOE
IOWA STATE UNIVERSITY
ATTN DR. K. A. GSCHNEIDNER, JR.
AMES, IA 50011

ARGONNE NATIONAL LABORATORY
ATTN DR. W. T. CARNALL
ATTN DR. H. M. CROSSWHITE
9700 SOUTH CASS AVENUE
ARGONNE, IL 60439

ARIZONA STATE UNIVERSITY
DEPT OF CHEMISTRY
ATTN DR. L. EYRING
TEMPE, AZ 85281

CARNEGIE MELLON UNIVERSITY
SCHENLEY PARK
ATTN PHYSICS & EE, DR. J. O. ARTMAN
PITTSBURGH, PA 15213

ENGINEERING SOCIETIES LIBRARY
ATTN ACQUISITIONS DEPT
345 EAST 47TH STREET
NEW YORK, NY 10017

HUGHES RESEARCH LAB
ATTN DR. L. G. DESHAZER
3011 MALIBU CANYON RD
MALIBU, CA 90265

JOHNS HOPKINS UNIVERSITY
DEPT OF PHYSICS
ATTN PROF. B. R. JUDD
BALTIMORE, MD 21218

KALAMAZOO COLLEGE
DEPT OF PHYSICS
ATTN PROF K. RAJNAK
KALAMAZOO, MI 49007

DIRECTOR
LAWRENCE RADIATION LABORATORY
ATTN DR. MARVIN J. WEBER
ATTN DR. HELMUT A. KOEHLER
ATTN DR. W. KRUPKE
LIVERMORE, CA 94550

MARTIN MARIETTA
ATTN DR. F. CROWNE
103 CHESAPEAKE PARK PLAZA
BALTIMORE, MD 21220

MASSACHUSETTS INSTITUTE OF TECHNOLOGY
CRYSTAL PHYSICS LABORATORY
ATTN DR. H. P. JENSSEN
ATTN B. AULL
ATTN DR. A. LINZ
CAMBRIDGE, MA 02139

MIT LINCOLN LAB
PO BOX 73
ATTN DR. PETER MOULTON
LEXINGTON, MA 02173

DEPARTMENT OF MECHANICAL, INDUSTRIAL,
& AEROSPACE ENGINEERING
PO BOX 909
ATTN DR. S. TEMKIN
PISCATAWAY, NJ 08854

UNIVERSITY OF MICHIGAN
COLLEGE OF ENGINEERING NORTH CAMPUS
DEPARTMENT OF NUCLEAR ENGINEERING
ATTN DR. CHIHIRO KIKUCHI
ANN ARBOR, MI 48104

DISTRIBUTION (Cont'd)

NATIONAL OCEANIC & ATMOSPHERIC ADM
ENVIRONMENTAL RESEARCH LABS
ATTN LIBRARY, R-51, TECH RPTS
BOULDER, CO 80302

OAK RIDGE NATIONAL LABORATORY
ATTN DR. R. G. HAIRE
OAK RIDGE, TN 37830

OKLAHOMA STATE UNIVERSITY
DEPT OF PHYSICS
ATTN PROF R. C. POWELL
STILLWATER, OK 74078

PENNSYLVANIA STATE UNIVERSITY
MATERIALS RESEARCH LABORATORY
ATTN DR. W. B. WHITE
ATTN DR. B. K. CHANDRASEKHAR
UNIVERSITY PARK, PA 16802

PORTLAND STATE UNIVERSITY
ATTN DR. J. B. GRUBER
PORTLAND, OR 92707

SETON HALL UNIVERSITY
CHEMISTRY DEPARTMENT
ATTN DR. H. BRITTAIN
SOUTH ORANGE, NJ 07099

TELEDYNE BROWN ENGINEERING
CUMMINGS RESEARCH PARK
ATTN DR. MELVIN L. PRICE,
MS-44
HUNTSVILLE, AL 35807

UNION CARBIDE CORP
ATTN M. R. KOKTA
ATTN J. H. W. LIAW
750 SOUTH 32ND STREET
WASHOUGAL, WA 98671

UNIVERSITY OF VIRGINIA
DEPT OF CHEMISTRY
ATTN DR. F. S. RICHARDSON
ATTN DR. M. REID
CHARLOTTESVILLE, VA 22901

MR. MICHAEL GILDNER (10 COPIES)
6400 LAKELAND DRIVE
RALEIGH, NC 27612

US ARMY ELECTRONICS RESEARCH
& DEVELOPMENT COMMAND
ATTN COMMANDER, DRDEL-CG
ATTN TECHNICAL DIRECTOR, DRDEL-CT
ATTN PUBLIC AFFAIRS OFFICE, DRDEL-IN

HARRY DIAMOND LABORATORIES
ATTN D/TSO/DIVISION DIRECTORS
ATTN RECORD COPY, 81200
ATTN HDL LIBRARY, 81100 (3 COPIES)
ATTN HDL LIBRARY, 81100 (WOODBIDGE)
ATTN TECHNICAL REPORTS BRANCH, 31300
ATTN LEGAL OFFICE, 97000
ATTN S. ELBAUM, 97100
ATTN CHAIRMAN, EDITORIAL COMMITTEE
ATTN ZABLUDOWSKI, B., 47400 (GIDEP)
ATTN CHIEF, 00210
ATTN LANHAM, C., 00213
ATTN LIBELO, L., 11200
ATTN CHIEF, 13000
ATTN KULPA, S., 13300
ATTN NEMARICH, J., 13300
ATTN BRODY, P., 13200
ATTN DROPKIN, H., 13200
ATTN FELOCK, R., 13200
ATTN LITTLE, J., 13200
ATTN WORTMAN, D., 13200
ATTN SATTLER, J., 13200
ATTN SIMONIS, G., 13200
ATTN SIMPSON, T., 13200
ATTN TOBIN, M., 13200
ATTN WEBER, B., 13300
ATTN WORCHESKY, T., 13200
ATTN CHIEF, 15000
ATTN WILLIS, B., 47400
ATTN LEAVITT, R., 13200 (10 COPIES)
ATTN MORRISON, C., 13200 (10 COPIES)

DATE
ILME